Non-Hermitian dynamics for a two-spin system with $\mathcal{PT}$ symmetry

Stavros Komineas
Department of Mathematics and Applied Mathematics, University of Crete, 70013 Heraklion, Crete, Greece and Institute of Applied and Computational Mathematics, FORTH, 70013 Heraklion, Crete, Greece

(Received 15 August 2022; revised 9 March 2023; accepted 16 March 2023; published 29 March 2023)

A system of interacting spins that are under the influence of spin-polarized currents can be described using a complex functional, or a non-Hermitian (NH) Hamiltonian. We study the dynamics of two exchange-coupled spins on the Bloch sphere. In the case of currents leading to $\mathcal{PT}$ symmetry, an exceptional point that survives also in the nonlinear system is identified. The nonlinear system is bistable for small currents and it exhibits stable oscillating motion or it can relax to an equilibrium point. The oscillating motion of the two spins is akin to synchronized spin-torque oscillators. For the full nonlinear system, we derive two conserved quantities that furnish a geometric description of the spin trajectories in phase space and indicate stability of the oscillating motion. Our analytical results provide tools for the description of the dynamics of NH systems that are defined on the Bloch sphere.

DOI: 10.1103/PhysRevB.107.094435

I. INTRODUCTION

Effective non-Hermitian (NH) Hamiltonians [1,2] have been employed for the description of classical [3,4] and quantum systems [5,6] that are coupled to the environment by dissipative or other forces. The observation that NH Hamiltonians that are invariant under the combination of parity and time reversal ($\mathcal{PT}$) foster real spectra [5,7] has led to a series of theoretical and experimental studies. A significant amount of work has focused on optical systems with balanced gain and loss such as in optical beam propagation [8] and single-mode lasers [9]. More recently, magnetic systems with $\mathcal{PT}$ symmetry have been proposed [10–13] and systems with gain and loss [14–17], with the latter reports focusing on degeneracies, called exceptional points (EPs), in the spectrum of the linear system, were the sensitivity of the system is enhanced. Effects of EPs were demonstrated for magnonic systems which possess two different loss factors [18].

Spin systems are studied extensively in relation to magnetic materials [19] motivated by applications in magnetic recording, nanoscopic sensors, antennas [20], computing applications, and neural network implementations [21]. Probing ferromagnets (and other magnetic materials) is done most efficiently by spin torques that are due to a spin-polarized current. This acts on the magnetic moments in the material in a way that may combine energy gain and loss and it drives magnetization dynamics [22]. Spin-transfer torque nano-oscillators (STNOs) can be constructed that give rise to magnetization oscillators due to injection of dc spin-polarized current [23]. A $\mathcal{PT}$-symmetric system of this kind with a single spin was studied in Ref. [10]. The synchronization of chains of STNOs in order to produce large power is a main challenge in this area [24,25].

We propose a $\mathcal{PT}$-symmetric system of two interacting spins or magnetic moments that can realistically be constructed when we invoke suitable spin-torque effects. We show that this is described by a complex function instead of a real Hamiltonian. This gives a paradigm of a realistic nontrivial system on the Bloch sphere. We show that the nonlinear system exhibits oscillating motion that is connected with the real eigenvalues of the linearized system. As a consequence, in the case of ferromagnets, one can design an appropriate setup for obtaining large-amplitude synchronized magnetization oscillations. Furthermore, this method can be extended to a chain of spins or oscillators. For the full nonlinear system, we derive two conserved quantities that make an explicit connection between the NH system and the Hamiltonian one, while they also furnish a geometric description of the spin trajectories in phase space. The existence of conserved quantities indicates that magnetization oscillations of large amplitude are expected to be stable.

Spin systems are crucial for quantum computing, and observations on a $\mathcal{PT}$-symmetric single-spin system have been reported [26]. Furthermore, an effective spin Hamiltonian is obtained in various physical systems. An example is a spin Hamiltonian obtained for qubits in an exciton polariton condensate, which are externally controllable by applied laser pulses and are coupled via a coherent tunneling term [27]. Finally, it is well known that the possible quantum states for a single qubit can be represented on a Bloch sphere. Our analytical results on complex Hamiltonians could provide tools for a more complete and elegant description of the dynamics of interacting spins on the Bloch sphere in magnetic and other systems.

The paper is organized as follows. In Sec. II, we give the formulation of a spin system using a complex functional. In Sec. III, we give the complex function for a system of two spins coupled by exchange. In Sec. IV, we give analytically simple periodic solutions for the spin dynamics. In Sec. V, we derive two conserved quantities and give their geometric meaning. Section VI contains our concluding remarks.

II. A COMPLEX FUNCTION FOR SPINS

We consider a spin system described via the magnetization vector $\boldsymbol{m} = (m_x, m_y, m_z)$ assumed to have a fixed length normalized to unity, $|\boldsymbol{m}| = 1$. If E denotes the magnetic energy, the conservative torque on the magnetization is $\boldsymbol{f} = -\partial E/\partial \boldsymbol{m}$. A polarized spin current that is injected in the system may produce an additional torque and the normalized equation of motion is [22]

$$\frac{\partial \boldsymbol{m}}{\partial t} = \boldsymbol{m} \times \frac{\partial E}{\partial \boldsymbol{m}} + \alpha\, \boldsymbol{m} \times \frac{\partial \boldsymbol{m}}{\partial t} - \beta\, \boldsymbol{m} \times (\boldsymbol{m} \times \boldsymbol{p}), \tag{1}$$

where $\boldsymbol{p}$ is the spin current polarization, β is a parameter proportional to the polarized current, and we have included a Gilbert damping term with parameter α. In the case of a ferromagnetic material, the time variable is scaled to $1/(\gamma \mu_0 M_s)$ where M_s is the saturation magnetization and γ is the gyromagnetic ratio.

The stereographic projection from the unit sphere $|\boldsymbol{m}| = 1$ to the complex plane is given by the complex variable

$$\Omega = \frac{m_x + i m_y}{1 + m_z}. \tag{2}$$

This can be inverted to give the magnetization components

$$m_x = \frac{\Omega + \overline{\Omega}}{1 + \Omega\overline{\Omega}}, \quad m_y = \frac{1}{i}\frac{\Omega - \overline{\Omega}}{1 + \Omega\overline{\Omega}}, \quad m_z = \frac{1 - \Omega\overline{\Omega}}{1 + \Omega\overline{\Omega}}, \tag{3}$$

where the bar denotes complex conjugation. The stereographic projection variable will make manifest the non-Hermiticity of the model and it will be central in the formulation of the present work.

The equation of motion for Ω, equivalent to Eq. (1), reads

$$(i + \alpha)\, \dot{\Omega} = -\frac{1}{2}\, (1 + \Omega\overline{\Omega})^2 \left(\frac{\partial E}{\partial \overline{\Omega}} + i\beta\, \frac{\partial E_{\rm ST}}{\partial \overline{\Omega}} \right), \tag{4}$$

where we have defined the function

$$E_{\rm ST} = -\boldsymbol{m} \cdot \boldsymbol{p}. \tag{5}$$

Formula (4) suggests the definition of a complex function that includes the spin-torque term,

$$F = E + i\beta E_{\rm ST}, \tag{6}$$

so that the equation of motion for Ω takes the compact form

$$(i + \alpha)\, \dot{\Omega} = -\frac{1}{2}\, (1 + \Omega\overline{\Omega})^2\, \frac{\partial F}{\partial \overline{\Omega}}. \tag{7}$$

The function F will be called the complex Hamiltonian.

As a basic example, if we have an external magnetic field $\boldsymbol{h} = (0, 0, h)$ giving rise to the energy $E = -\boldsymbol{m} \cdot \boldsymbol{h}$, and the spin polarization is $\boldsymbol{p} = (0, 0, 1)$, then $F = -(h + i\beta) m_z$ and the equation of motion is

$$(i + \alpha)\, \dot{\Omega} = -(h + i\beta)\Omega. \tag{8}$$

III. TWO EXCHANGE-COUPLED SPINS

We proceed to consider two magnetization vectors or spins interacting via exchange. These may represent two domains or layers in a magnetic material [28], or two effective spins in another physical system.

We denote the two vectors by $\boldsymbol{m}_1, \boldsymbol{m}_2$ and assume that they have equal length, $|\boldsymbol{m}_1| = |\boldsymbol{m}_2| = 1$. Except for the exchange interaction, we include an easy-axis anisotropy along z, and an external field $\boldsymbol{h} = h\hat{\boldsymbol{e}}_z$. The energy is

$$E = -J\, \boldsymbol{m}_1 \cdot \boldsymbol{m}_2 - \frac{\kappa}{2}[(m_{1,z})^2 + (m_{2,z})^2] - h\,(m_{1,z} + m_{2,z}), \tag{9}$$

where $J > 0$, $\kappa > 0$ are the exchange and anisotropy parameters, respectively, and $m_{1,z}, m_{2,z}$ denote the z components of the two vectors. We further consider that spin-polarized currents are injected in the two domains $\boldsymbol{m}_1, \boldsymbol{m}_2$, with polarization in two opposite directions, $\boldsymbol{p} = \pm\hat{\boldsymbol{e}}_z$. (Such a strategy for achieving $\mathcal{PT}$ symmetry is mentioned in [3] and attributed to [29].) The opposite polarizations could be achieved, e.g., in the case of two coupled ferromagnetic layers, by injecting a current through the layer separating the two magnetic layers [15], or by two different currents through layers adjacent to each one of the magnetic layers. Spin current polarization with a component perpendicular to the sample plane was recently demonstrated [30,31]. The equations of motion are

$$\begin{aligned} \dot{\boldsymbol{m}}_1 &= -\boldsymbol{m}_1 \times \boldsymbol{f}_1 + \alpha \boldsymbol{m}_1 \times \dot{\boldsymbol{m}}_1 - \beta \boldsymbol{m}_1 \times (\boldsymbol{m}_1 \times \hat{\boldsymbol{e}}_z), \\ \dot{\boldsymbol{m}}_2 &= -\boldsymbol{m}_2 \times \boldsymbol{f}_2 + \alpha \boldsymbol{m}_2 \times \dot{\boldsymbol{m}}_2 + \beta \boldsymbol{m}_2 \times (\boldsymbol{m}_2 \times \hat{\boldsymbol{e}}_z), \end{aligned} \tag{10}$$

where the dot denotes time differentiation and the effective fields are

$$\begin{aligned} \boldsymbol{f}_1 &= -\frac{\partial E}{\partial \boldsymbol{m}_1} = J\boldsymbol{m}_2 + \kappa\, m_{1,z}\hat{\boldsymbol{e}}_z + h\,\hat{\boldsymbol{e}}_z, \\ \boldsymbol{f}_2 &= -\frac{\partial E}{\partial \boldsymbol{m}_2} = J\boldsymbol{m}_1 + \kappa\, m_{2,z}\hat{\boldsymbol{e}}_z + h\,\hat{\boldsymbol{e}}_z. \end{aligned}$$

We will assume in the following $h > 0$, $\beta > 0$. Positive parameter β means that spin torque forces $\boldsymbol{m}_1$ to the north pole and $\boldsymbol{m}_2$ to the south pole. Equations (10) have four fixed points. Two fixed points correspond to both $\boldsymbol{m}_1, \boldsymbol{m}_2$ pointing at the north or at the south pole,

$$\boldsymbol{m}_1 = \boldsymbol{m}_2 = \hat{\boldsymbol{e}}_z, \tag{P1}$$

$$\boldsymbol{m}_1 = \boldsymbol{m}_2 = -\hat{\boldsymbol{e}}_z, \tag{P2}$$

and two further fixed points correspond to the vectors pointing at opposite poles,

$$\boldsymbol{m}_1 = \hat{\boldsymbol{e}}_z, \quad \boldsymbol{m}_2 = -\hat{\boldsymbol{e}}_z, \tag{P3}$$

$$\boldsymbol{m}_1 = -\hat{\boldsymbol{e}}_z, \quad \boldsymbol{m}_2 = \hat{\boldsymbol{e}}_z. \tag{P4}$$

For the study of the stability of the fixed points as well as for using the concepts of non-Hermiticity, we proceed to the formulation of the system using the stereographic projections (2) of each of the spins, denoted by Ω_1, Ω_2. We write the complex Hamiltonian of Eq. (6) for the system of two spins,

$$\begin{aligned} F = &-J\, \boldsymbol{m}_1 \cdot \boldsymbol{m}_2 - \frac{\kappa}{2}[(m_{1,z})^2 + (m_{2,z})^2] \\ &- h\,(m_{1,z} + m_{2,z}) + i\beta\,(m_{2,z} - m_{1,z}). \end{aligned} \tag{11}$$

This can be written in terms of the stereographic variables using Eqs. (3). For example, the exchange term is

$$-J\boldsymbol{m}_1 \cdot \boldsymbol{m}_2 = 2J\frac{(\Omega_1 - \Omega_2)(\overline{\Omega}_1 - \overline{\Omega}_2)}{(1 + \Omega_1\overline{\Omega}_1)(1 + \Omega_2\overline{\Omega}_2)}. \tag{12}$$

The equations of motion for Ω_1, Ω_2, from Eq. (7), read

$$(i+\alpha)\,\dot{\Omega}_1 = J\frac{1+\Omega_1\overline{\Omega}_2}{1+\Omega_2\overline{\Omega}_2}(\Omega_2-\Omega_1) - \kappa\frac{1-\Omega_1\overline{\Omega}_1}{1+\Omega_1\overline{\Omega}_1}\,\Omega_1 - (h+i\beta)\Omega_1,$$

$$(i+\alpha)\,\dot{\Omega}_2 = J\frac{1+\overline{\Omega}_1\Omega_2}{1+\Omega_1\overline{\Omega}_1}(\Omega_1-\Omega_2) - \kappa\frac{1-\Omega_2\overline{\Omega}_2}{1+\Omega_2\overline{\Omega}_2}\,\Omega_2 - (h-i\beta)\Omega_2. \tag{13}$$

System (13) is $\mathcal{PT}$-symmetric when we neglect the damping term by setting $\alpha = 0$. The terms with β act as gain and loss, but note that not each separate one of them can be classified as giving only gain or only loss. This is unlike in previous works on NH magnetics [14,15,17,32], where damping and antidamping torques were assumed [33].

The solution of Eq. (13) $\Omega_1 = 0$, $\Omega_2 = 0$ corresponds to the fixed point (P1) where both vectors point at the north pole. We can study the behavior of the system close to the fixed point if we assume $|\Omega_1|, |\Omega_2| \ll 1$ and linearize the equations. We have the linearized system (for $\alpha = 0$)

$$i\dot{\Omega}_1 = -(\omega_0+i\beta)\Omega_1 + J\Omega_2, \quad \omega_0 = J+\kappa+h,$$

$$i\dot{\Omega}_2 = -(\omega_0-i\beta)\Omega_2 + J\Omega_1 \tag{14}$$

that has the form of a standard linear $\mathcal{PT}$-symmetric dimer model. For $\beta \leqslant J$, we define an angle θ via

$$\sin\theta = \frac{\beta}{J}, \quad 0 \leqslant \theta \leqslant \pi, \tag{15}$$

and have the solution

$$\Omega_1 = A\,e^{i\omega t}, \quad \Omega_2 = A\,e^{i\theta}\,e^{i\omega t}, \tag{16}$$

with angular frequency

$$\omega = \omega_0 - J\cos\theta. \tag{17}$$

For every $\beta \leqslant J$, Eq. (15) gives two angles θ_1, θ_2 with $\theta_2 = \pi - \theta_1$ (assuming $\theta_1 < \pi/2$) and thus two frequency values are given by Eq. (17). For $0 \leqslant \theta = \theta_1 \leqslant \pi/2$, we obtain an acoustic branch and for $\pi/2 \leqslant \theta = \theta_2 \leqslant \pi$, we obtain an optical branch. States (16) correspond to periodic motion of both spins with equal amplitudes $|\Omega_1| = |\Omega_2|$. Equivalently, one can say that the spins have equal z components, $m_{1,z} = m_{2,z}$, while precession occurs around the z axis.

For $\beta > J$, the angular frequency has an imaginary part,

$$\omega = \omega_0 \pm iJ\sqrt{(\beta/J)^2-1}, \tag{18}$$

which means that $|\Omega_1|, |\Omega_2|$ will generically grow in time and, thus, the fixed point is unstable. A corresponding analysis for the fixed point (P2) gives the same stability results, that is, precessional motion for $\beta \leqslant J$ and an instability for $\beta > J$.

In order to study the fixed point (P3), we use the transformation $\Psi_2 = 1/\overline{\Omega}_2$ for the second spin. Then, (P3) corresponds to $\Omega_1 = 0$, $\Psi_2 = 0$. The equations of motion (13) become (for $\alpha = 0$)

$$i\,\dot{\Omega}_1 = J\frac{1-\Omega_1\overline{\Psi}_2}{1+\Psi_2\overline{\Psi}_2}(\Omega_1+\Psi_2) - \kappa\frac{1-\Omega_1\overline{\Omega}_1}{1+\Omega_1\overline{\Omega}_1}\,\Omega_1 - (h+i\beta)\Omega_1,$$

TABLE I. Stability regimes for the four fixed points. The results of linear stability analysis agree with numerical simulation results for the nonlinear system. We are confined to the case J, $\beta > 0$.

	Stable	Unstable
P1	$\beta \leqslant J$	$\beta > J$
P2	$\beta \leqslant J$	$\beta > J$
P3	$\kappa \geqslant 2J$ or $\beta \geqslant \sqrt{\kappa(2J-\kappa)}$	$\kappa < 2J$ and $\beta < \sqrt{\kappa(2J-\kappa)}$
P4		$\beta > 0$

$$i\,\dot{\Psi}_2 = J\frac{\overline{\Omega}_1\Psi_2-1}{1+\Omega_1\overline{\Omega}_1}(\Omega_1+\Psi_2) - \kappa\frac{\Psi_2\overline{\Psi}_2-1}{\Psi_2\overline{\Psi}_2+1}\,\Psi_2 - (h+i\beta)\Psi_2. \tag{19}$$

In order to study stability, we assume $\Omega_1, \Psi_2 \ll 1$ and linearize the equations to obtain

$$i\dot{\Omega}_1 = (J-\kappa-h-i\beta)\Omega_1 + J\Psi_2,$$

$$i\dot{\Psi}_2 = (-J+\kappa-h-i\beta)\Psi_2 - J\Omega_1. \tag{20}$$

Assuming solutions

$$\Omega_1 = A_1 e^{i\omega t}, \quad \Psi_2 = \frac{1}{\overline{\Omega}_2} = A_2 e^{i\omega t},$$

we obtain the condition

$$(\omega - h - i\beta)^2 = \kappa(\kappa - 2J). \tag{21}$$

In the case

$$\kappa \geqslant 2J \Rightarrow \omega = h \pm \sqrt{\kappa(\kappa-2J)} + i\beta, \tag{22}$$

we have that $i\omega$ has a negative real part, $-\beta$, giving asymptotic stability for every $\beta > 0$. In the case

$$\kappa < 2J \Rightarrow \omega = h + i[\beta \pm \sqrt{\kappa(2J-\kappa)}], \tag{23}$$

we have that

$$\beta \geqslant \sqrt{\kappa(2J-\kappa)} \tag{24}$$

gives asymptotic stability, while

$$\beta < \sqrt{\kappa(2J-\kappa)} \tag{25}$$

gives instability. The right side in Eq. (23) has a maximum equal to J at $\kappa = J$. This means that, for $\beta > J$, the fixed point is stable for every value of κ.

Finally, for the fixed point (P4), we can follow a similar procedure and find that it is unstable for every value of $\beta > 0$, $\kappa > 0$. This is a consequence of the fact that our choice of positive β forces $\boldsymbol{m}_1, \boldsymbol{m}_2$ away from the south and north pole, respectively; that is, it forces the system away from point (P4). Table I summarizes the results for the stability of the fixed points.

The linear stability results of this section determine cases where fixed points are unstable. On the other hand, in the cases where the linear system is stable (with a real frequency), no conclusive result can be drawn for the nonlinear system (as dictated by standard dynamical systems theory). Further study of the stability will be given in Sec. IV B.

IV. NONLINEAR OSCILLATIONS

A. Amplitude and frequency

We proceed to study solutions of the nonlinear system (13). We start by assuming solutions of the form (16) that is, perfect oscillations where the two spins differ by a phase. Substituting in Eqs. (13), we obtain

$$|A|^2[J(1-e^{-i\theta})+\kappa+\omega-h-i\beta] + [J(e^{i\theta}-1)-\kappa+\omega-h-i\beta]=0,$$
$$|A|^2[J(1-e^{i\theta})+\kappa+\omega-h+i\beta] + [J(e^{-i\theta}-1)-\kappa+\omega-h+i\beta]=0.$$

The two equations are identical if condition (15) holds, and they reduce to

$$|A|^2[J(1-\cos\theta)+\kappa+(\omega-h)] + [J(1-\cos\theta)+\kappa-(\omega-h)]=0.$$

This obtains the angular frequency as a function of the amplitude (as expected for nonlinear oscillators),

$$\omega=\frac{1-|A|^2}{1+|A|^2}[J\,(1-\cos\theta)+\kappa]+h. \tag{26}$$

For the interpretation of this result, one should note that $(1-|A|^2)/(1+|A|^2)$ gives the z component of $\boldsymbol{m}_1, \boldsymbol{m}_2$. Similarly to the linear case, we have an acoustic and an optical branch for nonlinear magnetization oscillations. Their frequencies are given by Eq. (26) for the two solutions $\theta=\theta_1,\theta_2$ of Eq. (15). Related observations were reported in [18] for a passive magnonic system.

Equation (15) implies an exceptional point at $\beta=J$ for the nonlinear system. This means that the system possesses periodic orbits for $\beta<J$ but these are not sustained for $\beta>J$. Furthermore, at $\beta=J$, Eq. (15) gives a single solution $\theta=\pi/2$; the two frequencies coalesce to a single one and we have only one nonlinear oscillation solution (16). The exceptional point of the nonlinear system coincides with that obtained for the linearized system (14). The stability of the periodic orbits in the nonlinear system will be studied numerically in the next subsection.

We conclude the subsection by making some further remarks on Eq. (26) and assuming $h=0$ for simplicity. The frequency is invariant under the transformation $A\to 1/A$. This corresponds to the invariance of the model under the transformation $m_3\to -m_3$. For small amplitude, $|A|\to 0$, the spins are close to the north pole of the Bloch sphere and Eq. (26) reduces to the result (17) of the linear model. The limit $|A|\to\infty$ is allowed and it corresponds to the spins being close to the south pole of the sphere. The frequency of oscillation has maximum absolute value for $\boldsymbol{m}$ close to the north ($A\to 0$) or the south pole ($|A|\to\infty$).

In the case that both spins point on the equator, $|A|=1$, there is no spin precession, $\omega=0$, according to Eq. (26) for $h=0$. Therefore, the configurations $\Omega_2=e^{i\theta}\Omega_1$, for $|\Omega_1|=|\Omega_2|=1$, give a continuum of fixed points of the system. These are additional to the four fixed points P1–P4 discussed in Sec. III. The new fixed points are obviously unstable, as any deviation from the equator would result in spin precession around the z axis, which means, the spins would go away from their fixed-point positions.

B. Numerics

We simulate numerically the system when it is below the exceptional point, for $\beta<J$, and find that it follows the precessional eigenstates (16) of the nonlinear system if the initial spin configuration is prepared so that it agrees with Eqs. (15) and (16). Figure 1(a) shows an example of spin precession for the acoustic branch. Figure 1(c) shows an example of spin precession for the optical branch. The graphs show the x and the z components of the magnetization vector. The frequency of precession is given by Eq. (26) and the result is verified in the graphs by the periodicity of the x components of the magnetization vectors.

Furthermore, for an initial condition that is close to the eigenstate (16), we obtain quasiperiodic motion where the z components of the spins oscillate while the spins precess around the z axis. An example is shown in Fig. 1(b), for an initial condition close to the one that gave the acoustic branch periodic motion in Fig. 1(a). Another example is shown in Fig. 1(d), for an initial condition close to the one that gave the optical branch periodic motion in Fig. 1(c). Two frequencies are involved in this motion. The precessional motion frequency is close to (26), while the periodicity of the oscillation of the z component of the spin gives a second frequency apparently unrelated to the spin precession frequency.

For the simulations in Fig. 1, we have chosen parameters such that condition (24) is satisfied, and the system is expected to be bistable as inferred from Table I. We run a further simulation using the same parameter set, but now choosing an initial condition close to the point (P3). We find that the system goes asymptotically to this fixed point, as shown in Fig. 2. This verifies the bistability of the system.

In the case that β satisfies condition (25), only (P1), (P2) are stable. Starting from any initial condition the system goes into a periodic or a quasiperiodic motion similar to those shown in Fig. 1.

Finally, when we cross the exceptional point, for $\beta>J$, the fixed points (P1), (P2) are unstable due to the imaginary part in the eigenvalues (18). Then, (P3) is the only stable fixed point and the system goes to that asymptotically from any initial condition.

We conclude the section with a note about the remarkable periodicity in the dynamics of this system. The quasiperiodic motion observed in many of the simulations cannot be considered as a direct consequence of the results obtained in Sec. III for the linearized equations. It is rather due to a partial or complete integrability of the system. The periodic and quasiperiodic dynamics can be anticipated due to the existence of the integrals that will be given in Sec. V.

V. CONSERVED QUANTITIES

A. Energy and magnetization

The existence of integrals of motion is implied by the correspondence between the $\mathcal{PT}$-symmetric Hamiltonian with a Hermitian one [34]. This is further supported by the existence of periodic and quasiperiodic solutions of the system of equations (10). It has been shown that a class of $\mathcal{PT}$-symmetric

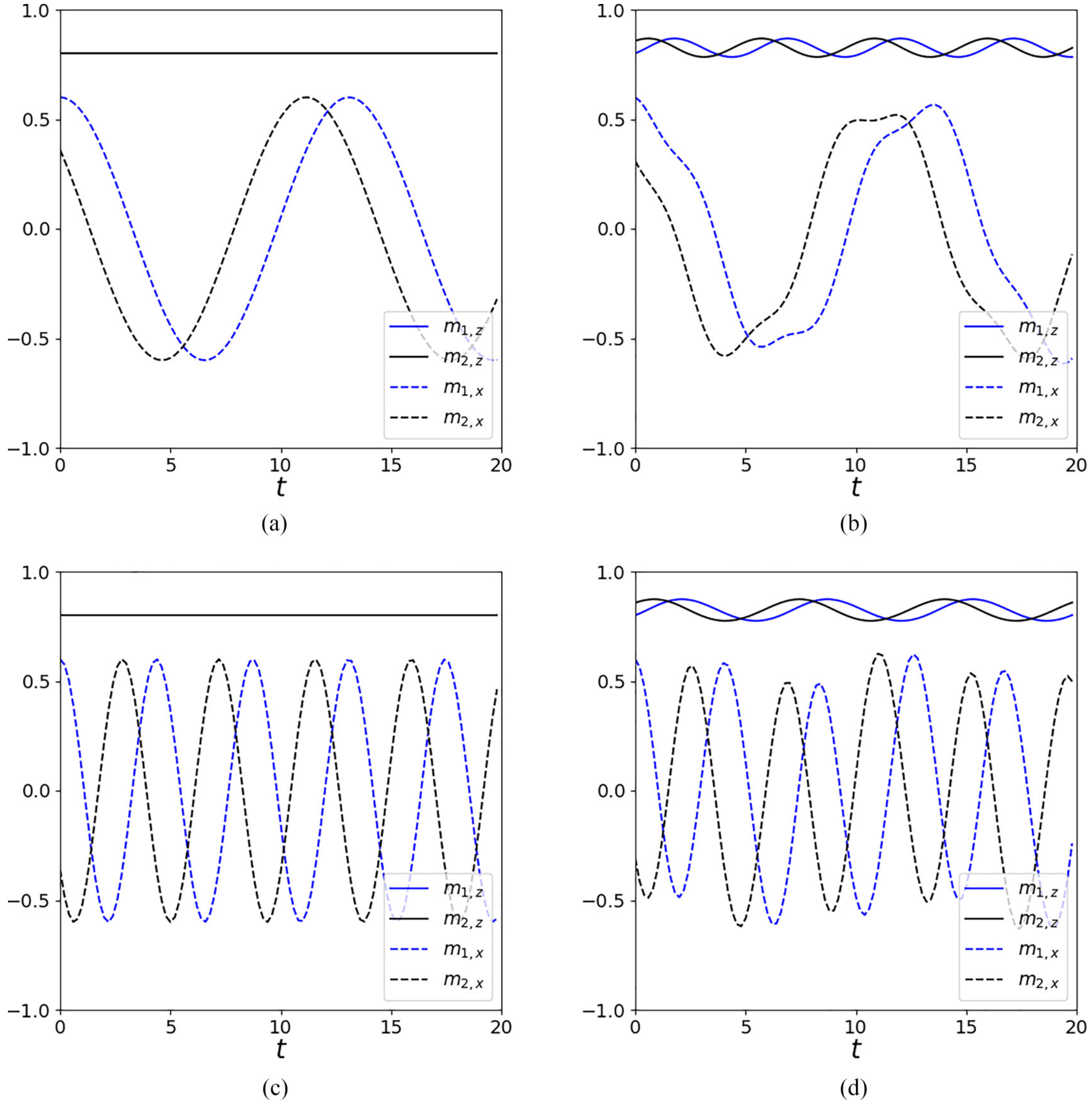

FIG. 1. We simulate Eqs. (13) with parameters $J = 1$, $\kappa = 0.2$, $h = 0$ and spin-torque parameter $\beta = 0.8$. The first and the third components of the magnetization $m_{1,x}(t)$, $m_{2,x}(t)$ and $m_{1,z}(t)$, $m_{2,z}(t)$ are shown. (a) Using an initial condition that agrees with Eqs. (15) (for $\theta < \pi/2$) and (16), we obtain spin precession in the acoustic branch, that is, oscillations around the nonlinear eigenstate (16). (b) When we choose the initial condition close to the values used in (a), we obtain oscillations of the z component of the spins in addition to precessional motion. (c) Using an initial condition that agrees with Eqs. (15) (for $\theta > \pi/2$) and (16), we obtain spin precession in the optical branch. (d) Similar simulation to (b) for the optical branch.

nonlinear Schrödinger dimers admit a Hamiltonian and are completely integrable systems [35–37].

We will derive integrals of motion for the undamped ($\alpha = 0$) system. We start by noting that, in the absence of spin torque ($\beta = 0$), the energy (9) and also the total magnetization along the symmetry axis

$$M_z = m_{1,z} + m_{2,z} \tag{27}$$

are conserved quantities. When $\beta \neq 0$, the time derivative of the energy is

$$\frac{dE}{dt} = -\beta\left(E - J - \frac{\kappa}{2}M_z^2 + \kappa\right)M^- \tag{28}$$

and the time derivative of M_z is

$$\frac{dM_z}{dt} = -\beta\, M_z M^-, \tag{29}$$

where we have defined the quantity

$$M^- = m_{1,z} - m_{2,z} \tag{30}$$

that will enter many calculations in this section.

Equations (28), (29) suggest that we define the quantity

$$G = E - J + \frac{\kappa}{2}\left(M_z^2 + 2\right), \tag{31}$$

whose time derivative has the form

$$\frac{dG}{dt} = -\beta\, G M^-. \tag{32}$$

Equation (32) together with Eq. (29) give the conserved quantity

$$I_1 = \frac{E - J + \frac{\kappa}{2}\left(M_z^2 + 2\right)}{M_z}. \tag{33}$$

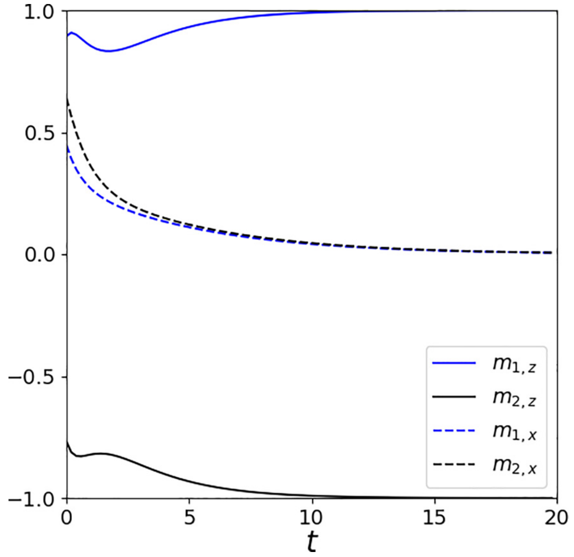

FIG. 2. We use the same parameter values as in the simulation in Fig. 1 so that $\beta > \sqrt{\kappa(2J-\kappa)} = 0.6$. We use an initial condition close to the fixed point (P3). We observe that the system goes asymptotically to this fixed point.

We can make further progress if we now confine ourselves to the *exchange model*, i.e., $\kappa = 0$. We have the conserved quantity

$$I_1 = \frac{E_{\rm ex} - J}{M_z}. \tag{34}$$

This is valid also in the presence of a field, $h \neq 0$.

B. Exchange model, first integral

We will proceed by using the Stokes variables defined as

$$S_0 = |\Omega_1|^2 + |\Omega_2|^2, \quad S_3 = |\Omega_1|^2 - |\Omega_2|^2, \\ S_1 + iS_2 = 2\overline{\Omega}_1\Omega_2. \tag{35}$$

The following result will prove central,

$$\frac{d}{dt}(S_1 + iS_2) = -\frac{iJ}{4} M^- (S_1 + 2 + iS_2)^2. \tag{36}$$

If we define $w = S_1 + 2 + iS_2$, then Eq. (36) is

$$\frac{dw}{dt} = i\gamma\, w^2, \tag{37}$$

where γ is implicitly defined. This equation gives invariant circles $w\bar{w} - R(w + \bar{w}) = 0$, or

$$(S_1 + 2 - R)^2 + S_2^2 = R^2, \tag{38}$$

where $R \in \mathbb{R}$ is an arbitrary constant. Figure 3 shows examples of these circles. Solving for R, we find that a conserved quantity is explicitly written as

$$\frac{(S_1+2)^2 + S_2^2}{S_1 + 2} = 2R. \tag{39}$$

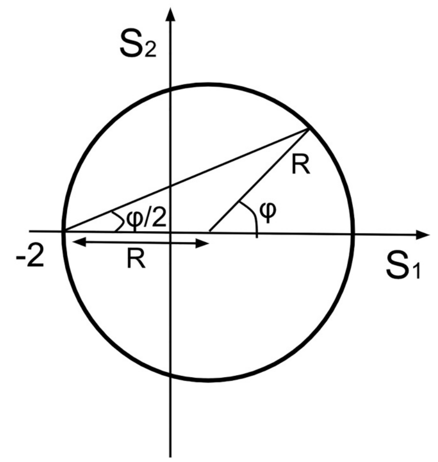

FIG. 3. The geometry of Eq. (38) and Eq. (41). Note that R may also be negative (then the center of the circle would be at $S_1 < -2$).

Equation (39) reproduces the result in Eq. (34). In order to see this, we write (34) in terms of the Stokes variables,

$$I_1 = J\frac{(S_1+2)^2 + S_2^2}{S_1^2 + S_2^2 - 4}. \tag{40}$$

Both Eqs. (39) and (40) are quadratic in S_1, S_2, and they give the same family of circles.

We conclude this subsection with some remarks. The point $S_1 + iS_2 = -2$ has a special role in this formulation, as it gives a fixed point of Eq. (36). It corresponds to $\overline{\Omega}_1\Omega_2 = -1 \Leftrightarrow \boldsymbol{m}_1 = -\boldsymbol{m}_2$.

If we consider anisotropy $\kappa \neq 0$, the integral (33) does not represent simply a curve on the (S_1, S_2) plane but a more complicated surface in the space (S_1, S_2, S_3).

A comparison of the results of the present section can be made with the more extensively studied system of two coupled nonlinear Schrödinger equations with cubic nonlinearity. The system has two conserved quantities that were reported in [38], and more extensively explained in Refs. [39–41]. A calculation similar to that in Eq. (36) gives a form $dw/dt = i\gamma'\, w$ with γ' some quantity independent of w; cf. Eq. (37). The solutions are a family of circles with the center at the origin of the plane (S_1, S_2).

C. Exchange model, second integral

We write Eq. (38) in the parametric form

$$S_1 + iS_2 = R - 2 + Re^{i\phi}, \quad 0 \leqslant \phi < 2\pi, \tag{41}$$

whose geometric meaning is shown in Fig. 3. We substitute Eq. (41) in Eq. (36) and obtain

$$\frac{d}{dt}[\tan(\phi/2)] = \frac{R}{2}J\,M^-. \tag{42}$$

Equation (42) gives the rate at which we move on a circle defined in Eq. (38). An example of the trajectory during the motion on the (S_1, S_2) plane is shown in Fig. 4.

We can now combine Eq. (42) with Eq. (29) and obtain a second conserved quantity

$$I_2 = \tan(\phi/2) + \frac{R}{2}\frac{J}{\beta}\ln|M_z|. \tag{43}$$

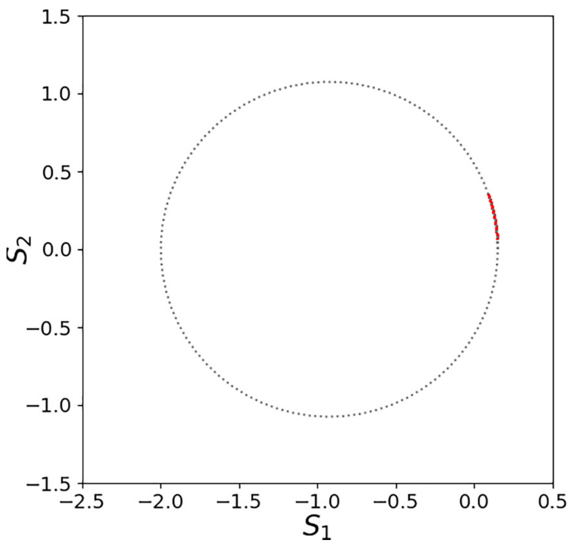

FIG. 4. We simulate Eqs. (13) with parameters $J=1$ and $\beta=0.8$ (we set $\kappa = 0$, $h = 0$, and $\alpha = 0$). The gray dotted line shows the circle (39) and the red arc shows the trajectory on the (S_1, S_2) plane. All Stokes variables present oscillating motion in time (not shown).

In Fig. 3, we see that

$$\tan(\phi/2) = \frac{\sin\phi}{1+\cos\phi} = \frac{S_2}{S_1+2},$$

and the conserved quantity (43) is written in terms of the Stokes variables as

$$I_2 = \frac{S_2}{S_1+2} + \frac{R}{2}\frac{J}{\beta}\ \ln\left|2\frac{4-\left(S_1^2+S_2^2\right)}{(S_0+2)^2-S_3^2}\right|, \tag{44}$$

where we have used

$$M_z = 2\frac{4-S_0^2+S_3^2}{(S_0+2)^2-S_3^2} = 2\frac{4-\left(S_1^2+S_2^2\right)}{(S_0+2)^2-S_3^2}.$$

The integral (44) could also be obtained by a combination of Eqs. (29) and (36). However, the method used in this subsection is a more transparent one as it is based on geometric arguments.

Finally, we note that if the system of equations could be produced by a Hamiltonian, the existence of the two integrals of motion would imply its complete integrability [37].

VI. CONCLUDING REMARKS

A system of interacting spins that are under spin-transfer torque can be described by a complex function, or a non-Hermitian Hamiltonian. We give the formalism for obtaining the complex function that makes manifest the $\mathcal{PT}$ symmetry when this is present. We have studied the nonlinear dynamics and the exceptional point for a system of two exchange-coupled spins in a case of $\mathcal{PT}$ symmetry. This introduces a paradigm for the dynamics of non-Hermitian systems defined on the sphere.

We have identified the regime for periodic precessional motion of the two spins, and its stability. The periodic motion corresponds to a locking of the complete system in sustained magnetization oscillations. The synchronization of the oscillations of the two spins, due to $\mathcal{PT}$ symmetry, could lead to an answer to the long-standing problem of the synchronization of spin-transfer torque nano-oscillators (STNOs) [24,25]. The rich spin dynamics for the spin system can be further used to study nonmagnetic systems which are described by effective spin variables (e.g., as in polariton condensates [27]).

The identification of conserved quantities in the system offers an explanation for the numerical observation of stable oscillatory behavior also in the nonlinear system. This finding will have consequences for NH magnonics if the method could be generalized to a chain of spins. We have found one conserved quantity in the general case. In the exchange model, a second one is found by exploiting the simple form of the first conserved quantity. In the general case, for nonzero anisotropy, it is likely that a second conserved quantity exists. It appears, however, technically difficult to identify its analytical form.

The present work introduces a NH system of interacting spins based on the standard modeling for the effect of spin torques in magnetic materials, i.e., including the Slonczewski spin-torque term in the interacting spins dynamics. It is thus amenable to realistic extensions that will possibly include further energy gain and loss effects, to layered systems (or a spin chain) with different gain and loss properties in the layers, and to NH magnonics.

ACKNOWLEDGMENTS

The author is grateful to Kostas Makris for discussions and insightful remarks. This work was supported by the project "ThunderSKY" funded by the Hellenic Foundation for Research and Innovation and the General Secretariat for Research and Innovation, under Grant No. 871.

[1] R. El-Ganainy, K. G. Makris, M. Khajavikhan, Z. H. Musslimani, S. Rotter, and D. N. Christodoulides, Non-Hermitian physics and PT symmetry, Nat. Phys. **14**, 11 (2018).
[2] E. J. Bergholtz, J. C. Budich, and F. K. Kunst, Exceptional topology of non-Hermitian systems, Rev. Mod. Phys. **93**, 015005 (2021).
[3] V. V. Konotop, J. Yang, and D. A. Zezyulin, Nonlinear waves in $\mathcal{PT}$-symmetric systems, Rev. Mod. Phys. **88**, 035002 (2016).
[4] M.-A. Miri and A. Alù, Exceptional points in optics and photonics, Science **363**, eaar7709 (2019).
[5] C. M. Bender, Making sense of non-Hermitian Hamiltonians, Rep. Prog. Phys. **70**, 947 (2007).
[6] I. Rotter, A non-Hermitian Hamilton operator and the physics of open quantum systems, J. Phys. A: Math. Theor. **42**, 153001 (2009).
[7] C. M. Bender and S. Boettcher, Real Spectra in Non-Hermitian Hamiltonians Having $\mathcal{PT}$ Symmetry, Phys. Rev. Lett. **80**, 5243 (1998).

[8] C. E. Rüter, K. G. Makris, R. El-Ganainy, D. N. Christodoulides, M. Segev, and D. Kip, Observation of parity-time symmetry in optics, Nat. Phys. **6**, 192 (2010).
[9] L. Feng, Z. J. Wong, R.-M. Ma, Y. Wang, and X. Zhang, Single-mode laser by parity-time symmetry breaking, Science **346**, 972 (2014).
[10] A. Galda and V. M. Vinokur, Parity-time symmetry breaking in magnetic systems, Phys. Rev. B **94**, 020408(R) (2016).
[11] A. Galda and V. M. Vinokur, Linear dynamics of classical spin as Möbius transformation, Sci. Rep. **7**, 1168 (2017).
[12] A. Galda and V. M. Vinokur, Exceptional points in classical spin dynamics, Sci. Rep. **9**, 17484 (2019).
[13] I. V. Barashenkov and A. Chernyavsky, Stable solitons in a nearly PT-symmetric ferromagnet with spin-transfer torque, Physica D **409**, 132481 (2020).
[14] H. Yang, C. Wang, T. Yu, Y. Cao, and P. Yan, Antiferromagnetism Emerging in a Ferromagnet with Gain, Phys. Rev. Lett. **121**, 197201 (2018).
[15] X.-g. Wang, G.-h. Guo, and J. Berakdar, Enhanced Sensitivity at Magnetic High-Order Exceptional Points and Topological Energy Transfer in Magnonic Planar Waveguides, Phys. Rev. Appl. **15**, 034050 (2021).
[16] S. Wittrock, S. Perna, R. Lebrun, R. Dutra, R. Ferreira, P. Bortolotti, C. Serpico, and V. Cros, Exceptional points controlling oscillation death in coupled spintronic nano-oscillators, arXiv:2108.04804.
[17] K. Deng, X. Li, and B. Flebus, Exceptional points as signatures of dynamical magnetic phase transitions, Phys. Rev. B **107**, L100402 (2023).
[18] H. Liu, D. Sun, C. Zhang, M. Groesbeck, R. Mclaughlin, and Z. V. Vardeny, Observation of exceptional points in magnonic parity-time symmetry devices, Sci. Adv. **5**, eaax9144 (2019).
[19] A. Hubert and R. Schäfer, *Magnetic Domains* (Springer, Berlin, 1998).
[20] A. Fert, N. Reyren, and V. Cros, Magnetic skyrmions: Advances in physics and potential applications, Nat. Rev. Mater. **2**, 17031 (2017).
[21] J. Grollier, D. Querlioz, and M. D. Stiles, Spintronic nanodevices for bioinspired computing, Proc. IEEE **104**, 2024 (2016).
[22] D. V. Berkov and A. J. Miltat, Spin-torque driven magnetization dynamics: Micromagnetic modeling, J. Magn. Magn. Mater. **320**, 1238 (2008).
[23] S. E. Russek, W. H. Rippard, T. Cecil, and R. Heindl, Spin-transfer nano-oscillators, in *Handbook of Nanophysics Functional Nanomaterials*, edited by K. D. Sattler (CRC Press, Boca Raton, FL, 2010).
[24] A. A. Awad, P. Dürrenfeld, A. Houshang, M. Dvornik, E. Iacocca, R. K. Dumas, and J. Åkerman, Long-range mutual synchronization of spin Hall nano-oscillators, Nat. Phys. **13**, 292 (2017).
[25] R. Lebrun, S. Tsunegi, P. Bortolotti, H. Kubota, A. S. Jenkins, M. Romera, K. Yakushiji, A. Fukushima, J. Grollier, S. Yuasa, and A. V. Cros, Mutual synchronization of spin torque nano-oscillators through a long-range and tunable electrical coupling scheme, Nat. Commun. **8**, 15825 (2017).
[26] Y. Wu, W. Liu, J. Geng, X. Song, X. Ye, C.-K. Duan, X. Rong, and J. Du, Observation of parity-time symmetry breaking in a single-spin system, Science **364**, 878 (2019).
[27] S. Ghosh and T. C. H. Liew, Quantum computing with exciton-polariton condensates, npj Quantum Inf. **6**, 16 (2020).
[28] W. Legrand, D. Maccariello, F. Ajejas, S. Collin, A. Vecchiola, K. Bouzehouane, N. Reyren, V. Cros, and A. Fert, Room-temperature stabilization of antiferromagnetic skyrmions in synthetic antiferromagnets, Nat. Mater. **19**, 34 (2020).
[29] Yu. B. Gaididei (unpublished).
[30] A. Bose and D. C. Ralph, Tilted spin current generated by an antiferromagnet, Nat. Electron. **5**, 263 (2022).
[31] A. Bose, N. J. Schreiber, R. Jain, D.-F. Shao, H. P. Nair, J. Sun, X. S. Zhang, D. A. Muller, E. Y. Tsymbal, D. G. Schlom, and D. C. Ralph, Tilted spin current generated by the collinear antiferromagnet ruthenium dioxide, Nat. Electron. **5**, 267 (2022).
[32] J. M. Lee, T. Kottos, and B. Shapiro, Macroscopic magnetic structures with balanced gain and loss, Phys. Rev. B **91**, 094416 (2015).
[33] H. M. Hurst and B. Flebus, Perspective: Non-Hermitian physics in magnetic systems, J. Appl. Phys. **132**, 220902 (2022).
[34] A. Mostafazadeh, Exact *PT*-symmetry is equivalent to Hermiticity, J. Phys. A: Math. Gen. **36**, 7081 (2003).
[35] I. V. Barashenkov, Hamiltonian formulation of the standard $\mathcal{PT}$-symmetric nonlinear Schrödinger dimer, Phys. Rev. A **90**, 045802 (2014).
[36] I. V. Barashenkov and M. Gianfreda, An exactly solvable *PT*-symmetric dimer from a Hamiltonian system of nonlinear oscillators with gain and loss, J. Phys. A: Math. Theor. **47**, 282001 (2014).
[37] I. V. Barashenkov, D. E. Pelinovsky, and P. Dubard, Dimer with gain and loss: Integrability and *PT*-symmetry restoration, J. Phys. A: Math. Theor. **48**, 325201 (2015).
[38] H. Ramezani, T. Kottos, R. El-Ganainy, and D. N. Christodoulides, Unidirectional nonlinear $\mathcal{PT}$-symmetric optical structures, Phys. Rev. A **82**, 043803 (2010).
[39] I. V. Barashenkov, G. S. Jackson, and S. Flach, Blow-up regimes in the $\mathcal{PT}$-symmetric coupler and the actively coupled dimer, Phys. Rev. A **88**, 053817 (2013).
[40] J. Pickton and H. Susanto, Integrability of $\mathcal{PT}$-symmetric dimers, Phys. Rev. A **88**, 063840 (2013).
[41] P. G. Kevrekidis, D. E. Pelinovsky, and D. Y. Tyugin, Nonlinear dynamics in *PT*-symmetric lattices, J. Phys. A: Math. Theor. **46**, 365201 (2013).